

Available online at www.sciencedirect.com

# **ScienceDirect**





# Evaluation of a photo-initiated copper(I)-catalyzed azide-alkyne cycloaddition polymer network with improved water stability and high mechanical performance as an ester-free dental restorative



Xiance Wang<sup>a</sup>, Guangzhe Gao<sup>b</sup>, Han Byul Song<sup>a</sup>, Xinpeng Zhang<sup>a</sup>, Jeffrey W. Stansbury<sup>a,c</sup>, Christopher N. Bowman<sup>a,b,\*</sup>

- <sup>a</sup> Department of Chemical and Biological Engineering, University of Colorado Boulder, 596 UCB, Boulder, CO, United States
- <sup>b</sup> Materials Science and Engineering Program, University of Colorado Boulder, 596 UCB, Boulder, CO, United States
- <sup>c</sup> Department of Craniofacial Biology, School of Dental Medicine, Anschutz Medical Campus, Aurora, CO, United States

### ARTICLE INFO

Article history: Received 4 June 2021 Accepted 14 August 2021

Keywords:
Photopolymerization
CuAAC
Dental resins
Click chemistry
Step-growth polymerization

### ABSTRACT

Objective. The objective is to develop and characterize an ester-free ether-based photo-CuAAC resin with high mechanical performance, low polymerization-induced stress compared with common BisGMA/TEGDMA (70/30) resins, and improved water stability in comparison to previously developed urethane-based photo-CuAAC resins.

Methods. Triphenyl-ethane-centered ether-linked tri-azide monomers were synthesized and co-photopolymerized with ether-linked tri-alkyne monomers under visible light irradiation using a copper(II) pre-catalyst and CQ/EDAB as the initiator. The ether-based CuAAC formulation was investigated for thermo-mechanical properties, polymerization kinetics and shrinkage stress, and flexural properties with respect to a conventional BisGMA/TEGDMA (70/30) dental resin. In addition, both the ether-based CuAAC resin and the urethane-based CuAAC resin were examined for their water stability using the BisGMA/TEGDMA (70/30) resin as a control.

Results. The ether-based CuAAC network (AK/AZ-1) exhibited a slightly lower glass-transition temperature compared with the BisGMA/TEGDMA network (108 °C vs 128 °C), but because of its much sharper glass transition, the AK/AZ-1 CuAAC-network maintained storage modulus higher than 1 GPa up to 100 °C. In addition, the ether-based AK/AZ-1 network exhibited reduced shrinkage stress (0.56 MPa vs 1.0 MPa) and much higher flexural toughness (7.6 MJ/m³ vs 1.6 MJ/m³) while showing slightly lower flexural modulus and slightly higher flexural strength compared with the BisGMA/TEGDMA network. Moreover, the ether-based AK/AZ-1 CuAAC network displayed comparable water stability in comparison to the BisGMA/TEGDMA network with slightly higher water sorption (46  $\mu$ g/mm³ vs 38  $\mu$ g/mm³) and much lower water solubility (2.3  $\mu$ g/mm³ vs 4.4  $\mu$ g/mm³).

<sup>\*</sup> Corresponding author at: Department of Chemical and Biological Engineering, University of Colorado Boulder, 596 UCB, Boulder, CO, United States.

Significance. Employing the ether-based hydrophobic CuAAC formulation significantly improved the water stability of the CuAAC network compared with previously developed urethane-based CuAAC networks. Furthermore, compared with the conventionally used BisGMA/TEGDMA formulation, the reduced shrinkage stress, comparable flexural strength/flexural modulus, and the superior flexural toughness of the ether-based CuAAC network make it a promising ester-free alternative to the currently widely-used methacrylate-based dental restoratives.

© 2021 The Academy of Dental Materials. Published by Elsevier Inc. All rights reserved.

### 1. Introduction

Polymer-based dental restorative materials have, for decades, been primarily relying on di-methacrylate monomers, notably bisphenol A glycidyl methacrylate (BisGMA), triethylene glycol dimethacrylate (TEGDMA) and urethane dimethacrylate (UDMA) [1,2]. Among the advantages of poly(methacrylate) materials are their fast photo-curing kinetics, robust mechanical properties, and appealing aesthetic appearance [3-6]. However, drawbacks associated with chain-growth radical polymerization of methacrylate monomers persist. First, limited final conversions due to early vitrification raise toxicity concerns because the unreacted monomers in the resin matrices are potentially leachable [7]. Further, considerable polymerization-induced shrinkage stress develops [8-11], also because of the early gelation, during the photocuring of dimethacrylate monomers, and the high shrinkage stress can lead to failure of the restoratives, poor adhesion between restoratives and tooth [12]. Additionally, the ester groups within the backbone of the methacrylate monomers are prone to enzymatic hydrolysis [13,14], slowly reducing the mechanical properties of the restoratives in the long run and thus shortening their service lifetime and necessitating replacement of the restoratives [12]. Further, the potentially leachable degradation fragments also raise concerns of their toxicity [15–17]. Finally, the poly(methacrylate) materials are known for their brittleness, making them potentially prone to impact failures.

In the past two decades, several approaches have been explored to develop alternatives to the poly(methacrylate)based dental restoratives. For example, an epoxy-based siloxane/oxirane or silorane system was shown to generate lower shrinkage than di-methacrylate-based resins [18-20], likely due to the compensation effect resulting from the opening of the strained oxirane ring. Step-growth polymerizations such as radical-mediated thiol-ene photopolymerizations have received attention as alternative dental restorative materials in recent years [21-25] because of the robust photo-curing kinetics that are comparable to the free radical polymerizations of (meth)acrylates, the commercial availability of a wide range of both thiol and ene monomers, the reduced shrinkage stress due to delayed gelation in step-growth polymerizations, and the formation of more homogeneous and tougher networks because of the more uniform molecular weight buildup of the polymers. Efforts were also made to modify the di-methacrylate formulations, either by designing high molecular-weight and/or urethane-modified di-methacrylate monomers [26–29] or by incorporating reversible addition-fragmentation chain transfer (RAFT) moieties [30–32] into the monomer backbone to reduce polymerization shrinkage stress without sacrificing mechanical performance. Such efforts, however, only solve some of the problems associated with methacrylate-based systems as many of the problems are inherent to either methacrylate monomers (e.g., hydrolysis-prone esters) or to free radical chain-growth polymerizations.

As the prime example of click chemistry [33–35], the Cu(I)-catalyzed azide-alkyne cycloaddition (CuAAC) reaction has found a wide range of applications in bio-conjugations, material syntheses, surface functionalization, etc. ever since being discovered independently by the Meldal and the Sharpless laboratories [36,37]. Taking advantage of the reducing characteristics of photo-generated radicals, photo-initiated CuAAC reactions were realized in 2010 for the fabrication of patterned hydrogels [38] and for the formation of block copolymers [39], further expanding the application of CuAAC reactions by endowing the already-powerful click reaction with spatial and temporal control.

Recently, it has been demonstrated that photo-initiated step-growth CuAAC polymerization (Scheme 1), in contrast to chain-growth free-radical polymerizations of (meth)acrylates, afforded homogeneous glassy networks with robust mechanical properties, and with low polymerization-induced shrinkage stress due to delayed gelation [40,41], making the photocurable CuAAC resins a good candidate for esterfree dental restoratives. Furthermore, unlike most glassy thermosets, photo-CuAAC networks were shown to exhibit exceptionally high ductility and high tensile toughness in the glassy state [42].

In the present work, we further the development of the photo-CuAAC polymerization for its potential dental restorative application by designing new monomers and examining the polymerized networks' mechanical performance and water stability. Here, using the BisGMA/TEGDMA (70/30) comonomer resin as a control, we show that the new CuAAC resin consisting of ether-based hydrophobic monomers, compared with previously reported urethane-based monomers, exhibited much improved water stability that is comparable to the BisGMA/TEGDMA resin. On top of the lower polymerization-induced shrinkage stress as previously observed with the photo-CuAAC resin, the mechanical properties of the CuAAC resin were also similar or superior in comparison to the BisGMA/TEGDMA (70/30) resin.

Scheme 1 – Photoinduced, radical-initiated CuAAC polymerization forming poly(triazole) networks employing a photo-initiator in conjunction with a coper(II) pre-catalyst.

# 2. Experimental section

### 2.1. Materials

1,3-Bis(2-isocyanatopropan-2-yl)benzene, dibutyltin dilaurate, tetrahydrofuran, 6-chloro-1-hexanol, 3-chloro-1-propanol, sodium azide, 1,1,1-tris(hydroxymethyl)propane, propargyl bromide, ethanol, copper(II) chloride, N,N,N',N',N''-pentamethyldiethylenetriamine (PMDETA), camphorquinone (CQ), ethyl 4-(dimethylamino)benzoate (EDAB), and acetonitrile were used as received from Sigma Aldrich. Sodium hydroxide, ammonium chloride, dimethyl sulfoxide, dimethylformamide, methanol, and sodium sulfate were used as received from Fisher Scientific. BisGMA/TEGDMA (70/30) comonomers solution was used as received from ESSTECH. Bis(6azidohexyl) (1,3-phenylenebis(propane-2,2-diyl))dicarbamate 1-(prop-2-yn-1-yloxy)-2,2-bis((prop-2-yn-1yloxy)methyl)butane (AK) were synthesized according to previously reported procedures [43]. All organic azides were synthesized according to the azide safety rules and handled with appropriate precaution [37] when working with monomers, resins, and polymers in small quantities.

### 2.1.1. Synthesis of

# 1,1,1-tris(4-(3-chloropropyl)phenyl)ethane intermediate

To a solution of 1,1,1-tris(4-hydroxyphenyl)ethane (10 mmol, 3.06 g), 3-chloro-1-propanol (45 mmol, 3.76 ml), and triphenylphosphine (31 mmol, 8.31 g) in anhydrous THF (100 ml) was added diethyl azodicarboxylate (14.13 ml, 40 wt.% in toluene) dropwise at 0 °C under nitrogen. The reaction mixture was then warmed to room temperature and stirred overnight. The reaction mixture was diluted with EtOAc (150 ml), washed with  $\rm H_2O$  (50 ml  $\times$  3), and then dried with  $\rm Na_2SO_4$ . The product was obtained after flash chromatography using a hexane/EtOAc (90:10) mixture as eluent, dried in vacuo as a white solid. (52% yield)  $^1\rm H$  NMR (CDCl<sub>3</sub>), ppm:  $\delta$  2.11 (3H, s, CH<sub>3</sub>), 2.23 (6H, q, CH<sub>2</sub>—CH<sub>2</sub>C—H<sub>2</sub>), 3.75 (6H, t, CH<sub>2</sub>C—l), 4.09 (6H, t, CH<sub>2</sub>—O), 6.77–6.81 (6H, m, CH-aromatic), 6.97–7.01 (6H, m, CH-aromatic);  $^{13}\rm C$  NMR (CDCl<sub>3</sub>), ppm:  $\delta$  30.79, 32.34, 41.62, 50.62, 64.12, 113.65, 129.65, 141.98, 156.71.

# 2.1.2. Synthesis of

# 1,1,1-tris(4-(3-azidopropyl)phenyl)ethane (AZ-1)

To a solution of 1,1,1-tris(4-(3-chloropropyl)phenyl)ethane (5.2 mmol, 2.79 g) in DMF (50 ml) was added sodium azide (46.8

mmol, 3.04 g). The reaction mixture was then heated to 80 °C and stirred overnight. The reaction mixture was diluted with EtOAc (150 ml), washed with H<sub>2</sub>O (50 ml  $\times$  3), and then dried with Na<sub>2</sub>SO<sub>4</sub>. The pure product was obtained after flash chromatography using a hexane/EtOAc (85:15) mixture as eluent, dried in vacuo as a colorless oil. (98% yield) <sup>1</sup>H NMR (CDCl<sub>3</sub>), ppm:  $\delta$  2.04 (6H, q, CH<sub>2</sub>C-H<sub>2</sub>C-H<sub>2</sub>), 2.10 (3H, s, CH<sub>3</sub>), 3.52 (6H, t, CH<sub>2</sub>N-3), 4.02 (6H, t, CH<sub>2</sub>-O), 6.76–6.80 (6H, m, CH-aromatic), 6.96–7.01 (6H, m, CH-aromatic); <sup>13</sup>C NMR (CDCl<sub>3</sub>), ppm:  $\delta$  28.83, 30.79, 48.28, 50.62, 64.35, 113.62, 129.66, 142.00, 156.67.

# 2.1.3. Synthesis of

# 1,1,1-tris(4-(6-chlorohexyl)phenyl)ethane intermediate

To a solution of 1,1,1-tris(4-hydroxyphenyl)ethane (10 mmol, 3.06 g), 6-chloro-1-hexanol (45 mmol, 6.0 ml), and triphenylphosphine (31 mmol, 8.31 g) in anhydrous THF (100 ml) was added diethyl azodicarboxylate (14.13 ml, 40 wt.% in toluene) dropwise at 0 °C under nitrogen. The cooled reaction mixture was then warmed to room temperature and stirred overnight. The reaction mixture was diluted with EtOAc (150 ml), washed with  $H_2O$  (50 ml  $\times$  3), and then dried with  $Na_2SO_4$ . The product was obtained after flash chromatography using a hexane/EtOAc (90:10) mixture as eluent, dried in vacuo as a colorless oil. (61% yield)  $^{1}$ H NMR (CDCl<sub>3</sub>), ppm:  $\delta$  1.46–1.58 (12H, m, CH<sub>2</sub>CH-<sub>2</sub>C-H<sub>2</sub>C-H<sub>2</sub>CH-<sub>2</sub>CH-<sub>2</sub>), 1.75-1.88 (12H, m,  $CH_2C-H_2CH-_2CH-_2C-H_2C-H_2$ ), 2.12 (3H, s,  $CH_3$ ), 3.57 (6H, t, CH<sub>2</sub>-Cl), 3.96 (6H, t, CH<sub>2</sub>-O), 6.76-6.83 (6H, m, CH-aromatic), 6.97–7.04 (6H, m, CH-aromatic);  $^{13}$ C NMR (CDCl<sub>3</sub>), ppm:  $\delta$  25.48, 26.68, 29.20, 32.54, 45.08, 50.56, 67.59, 113.54, 129.61, 141.73, 157.01.

### 2.1.4. Synthesis of

# 1,1,1-tris(4-(6-azidohexyl)phenyl)ethane (AZ-2)

To a solution of 1,1,1-tris(4-(6-chlorohexyl)phenyl)ethane (6.1 mmol, 4.04 g) in DMF (60 ml) was added sodium azide (48.8 mmol, 3.17 g). The reaction mixture was then heated to 80 °C and stirred overnight. The cooled reaction mixture was diluted with EtOAc (2000 ml), washed with H<sub>2</sub>O (60 ml  $\times$  3), and then dried with Na<sub>2</sub>SO<sub>4</sub>. The pure product was obtained after flash chromatography using a hexane/EtOAc (90:10) mixture as eluent, dried in vacuo as a colorless oil. (95% yield)  $^1\text{H}$  NMR (CDCl<sub>3</sub>), ppm:  $\delta$  1.39–1.57 (12H, m, CH<sub>2</sub>CH–<sub>2</sub>C–H<sub>2</sub>C–H<sub>2</sub>CH–<sub>2</sub>CH–<sub>2</sub>CH–<sub>2</sub>C, 1.60–1.70 (6H, m, OCH–<sub>2</sub>CH–<sub>2</sub>CH–<sub>2</sub>CH–<sub>2</sub>CH–<sub>2</sub>CH–<sub>2</sub>CH–<sub>2</sub>N–<sub>3</sub>), 1.76–1.86 (6H, m, OCH–<sub>2</sub>C–H<sub>2</sub>CH–<sub>2</sub>CH–<sub>2</sub>CH–<sub>2</sub>CH–<sub>2</sub>N–<sub>3</sub>), 2.12 (3H, s, CH<sub>3</sub>), 3.31 (6H, t, CH<sub>2</sub>N–<sub>3</sub>), 3.96 (6H, t, CH<sub>2</sub>–O), 6.76–6.83 (6H, m, CH-aromatic), 6.96–7.03 (6H, m, CH-aromatic);  $^{13}\text{C}$  NMR (CDCl<sub>3</sub>),

ppm: δ 25.75, 26.54, 28.82, 29.22, 30.80, 50.56, 51.40, 67.58, 113.54, 129.61, 141.74, 157.01.

# 2.1.5. Preparation of CuCl<sub>2</sub>[PMDETA] complex

1:1 molar mixture of  $CuCl_2$  and PMDETA (N,N,N',N'',N''-1) pentamethyldiethylenetriamine) in acetonitrile was stirred overnight at room temperature and dried in vacuo to give a blue solid.

# Methods

### 3.1. Resin preparation

Stoichiometric mixtures of azide and alkyne monomers (functional group molar ratio of 1:1 N<sub>3</sub>/alkyne), and 1 mol% of CuCl<sub>2</sub>[PMDETA] per functional group, 0.68 wt.% of CQ, and 0.86 wt.% of EDAB were mixed, to which methanol (for AK/AZ-3 mixture) or methanol/acetone (for AK/AZ-1 and AK/AZ2 mixtures) was added to homogenize the mixture being later removed in vacuo. For the BisGMA/TEGDMA resin, to the BisGMA/TEGDMA (70/30) comonomer mixture was added 0.68 wt.% of CQ and 0.86 wt.% of EDAB and thoroughly stirred to afford the homogenous resin.

# 3.2. Fourier transform infrared spectroscopy

An FTIR spectrometer (Nicolet 6700) was used to monitor the real-time polymerization kinetics of the functional group conversion. Samples were placed between two cylindrical quartz rods, and light was irradiated through the bottom rod using a light guide connected to a mercury lamp (Acticure 4000, EXFO) with 400–500 nm bandgap filter, and the light intensity was set at 200 mW/cm<sup>2</sup>. A radiometer (Model 100, Demetron Research) was used to measure the output power density of the lamp. The overtone signal of the alkyne was monitored in the range of 6538–6455 cm<sup>-1</sup>, and the overtone signal of the methacrylate was measured in the range of 6250–6096 cm<sup>-1</sup>.

# 3.3. Polymerization shrinkage stress measurement

In situ polymerization shrinkage stress measurements were conducted with a tensometer (American Dental Association Health Foundation). Samples were sandwiched between the ends of 2 silanized glass rods (6 mm in diameter, 1 mm in thickness). The tensile force generated during photocuring by the bonded sample causes the cantilever beam to deflect. The deflection is measured by a linear variable differential transformer (LVDT) and then translated into the force based on the calibrated beam constant. To calculate the stress, the force corresponding to the beam deflection is divided by the cross-sectional sample area. The shrinkage stress was monitored from the start of light irradiation until 5 min after the light source was switched off to obtain the final shrinkage stress at ambient temperature. The irradiation time was 10 min, and the total measurement time was 15 min.

# 3.4. Dynamic mechanical analysis

A DMA Q800 (TA instruments) in multi-frequency-strain mode with frequency of 1 Hz and a heating rate of 3 °C min $^{-1}$  was used to measure the storage modulus and the glass transition temperature (Tg), which was assigned as the peak of the tan  $\delta$  (a ratio of E″/E′: the storage and loss moduli) curve. Film samples were irradiated with 12 mW cm $^{-2}$  of 400–500 nm visible light, via a light guide with a collimator connected to a mercury lamp (Acticure 4000, EXFO), for 5 min at room temperature on one side and immediately inverted to cure for another 5 min of the other side. The rectangular dimension of each sample specimen was 0.25  $\times$  5  $\times$  15 mm (t  $\times$  w  $\times$  l), and the samples were post-cured at 90 °C overnight.

### 3.5. Three-point flexural test

Three-point bending (MTS 858 Mini Bionix II) with a strain rate of 1 mm min $^{-1}$  and a span of 20 mm was used to obtain flexural modulus, flexural strength, and flexural toughness. Photo-activation provided 200 mW cm $^{-2}$  of 400–500 nm light from a mercury lamp (Acticure 4000, EXFO) by a light guide with a collimator. Samples were irradiated for 180 s at room temperature on one side followed by immediate inversion to cure for 180 s on the other side. The rectangular dimension of each sample specimen was 2  $\times$  2  $\times$  25 mm (t  $\times$  w  $\times$  l).

# 3.6. Water sorption/solubility tests

Water sorption tests were conducted using disc-shaped specimens of 1.2 mm in thickness and 12-13 mm in diameter. The samples were cured using 400-500 nm visible light (12 mW/cm<sup>2</sup>, 10 min for each side of the samples at room temperature) and were post-cured at 90 °C overnight. The samples obtained were dried in an oven at 37 °C until constant initial masses  $(m_i)$ . The thickness and diameter of each disc-shaped specimen were measured with calipers at 3-4 different positions to get averaged values and the initial volume (V<sub>i</sub>) of each specimen was calculated based on those values. The samples were then placed in distilled water at 37 °C. At regular time intervals (24 h), the samples were removed from the water, and the water on the surface of the samples was gently wiped away using Kimwipes. After their mass was recorded, the samples were returned to DI water for conditioning. The measurements were repeated until there was no significant change in mass for each specimen. This final mass of each specimen is referred to as the equilibrium saturation mass  $(m_s)$ . After determining the equilibrium saturation mass, the dimensions of each specimen were measured again, and the saturation volume was calculated (V<sub>s</sub>) in the same way the V<sub>i</sub> was calculated. Next, the samples were dried in an oven at 37 °C until constant mass, referred to as the desorption mass  $(m_d)$ . And the dimensions of the dried samples were measured again, and the dry volume was calculated  $(V_d)$  in the same way the V<sub>i</sub> and V<sub>s</sub> were calculated. The equilibrium solubility limit, s, and the equilibrium water sorption, w, were calculated according to the following equations [44]:

$$s(\mu g/mm^3) = (m_i - m_d)/V_i$$

Fig. 1 – Monomer libraries of tri-alkyne AK, tri-azides AZ-1 and AZ-2, di-azide AZ-3, di-methacrylates BisGMA and TEGDMA, and photo-initiator CQ, co-initiator EDAB, and copper(II) pre-catalyst CuCl<sub>2</sub>[PMDETA].

 $w(\mu g/mm^3) = (m_s - m_i)/V_i$ 

# 3.7. Statistical analysis

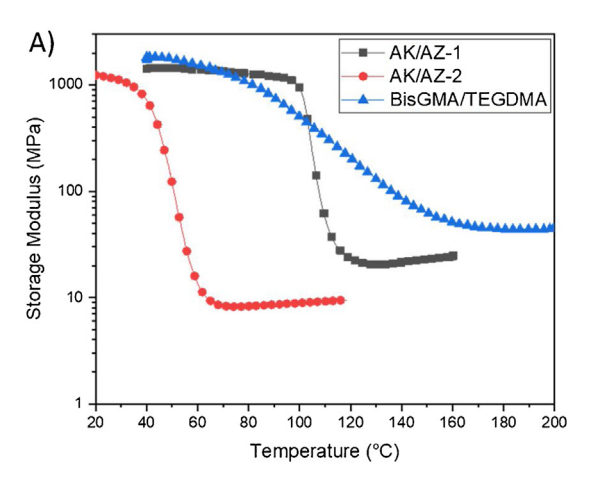
Statistical analysis of the experiments was performed via one-way analysis of variance (ANOVA), and multiple pairwise comparisons were conducted via Tukey's test with a significance level of 0.05. The number of repetitions for each experiment is as follow: dynamic mechanical analysis (n = 3), water sorption test (n = 5), three-point flexural test (n = 3).

# 4. Results and discussion

In the present study, triphenyl ethane-centered ether-linked tri-azides AZ-1 and AZ-2 (See Fig. 1 for the monomer structures, together with the initiator/co-initiator and copper pre-catalyst used) were designed as ester-free hydrophobic monomers and were synthesized simply with good overall yields. Photo-polymerization of either AZ-1 or AZ-2 with ether-linked tri-alkyne monomer AK formed a glassy network with glass-transition temperature (Tg) of 108 °C or 56 °C, respectively (Fig. 2B), as determined by dynamic mechanical analysis. The storage modulus (at 40 °C) of the AK/AZ-2 network was slightly below 1 GPa due to the proximity of the temperature (40 °C) to its glass-transition temperature, while the storage modulus of the AK/AZ-2 network was about 1.4 GPa (at 40 °C) which was slightly lower than that of the BisGMA/TEGDMA network. Both networks exhibited a sharp glass-transition, highlighting the more homogeneous networks of the chain-growth CuAAC polymerization in comparison to the BisGMA/TEGDMA network. Because of the sharp glass-transition, the AK/AZ-1 network maintained a storage modulus of higher than 1 GPa up to 100 °C, while the storage modulus of the BisGMA/TEGDMA network at 100 °C was significantly lower than 1 GPa despite having a higher glasstransition temperature (128 °C vs 108 °C). In addition to the relatively low glass-transition temperature, the photopolymerized AK/AZ-2 samples tend to have a lot of bubbles within it after photocuring and post-cure processing, which was detrimental for its potential application for dental restoratives

and made it impossible to run additional (flexural three-point bending and water sorption) tests with the AK/AZ-2 samples. The bubble issue is not uncommon with the photo-CuAAC polymerization, as it depends not only on the monomer structure but also on the photocuring conditions [45]. Thus, only AK/AZ-1 networks were studied further in terms of the photocuring kinetics, the photo-polymerization induced shrinkage stress, and the water sorption/solubility in comparison to the commercial dimethacrylate control. The previously investigated CuAAC resin [41] composed of urethane-linked di-azide monomer AZ-3 and tri-alkyne monomer AK was also assessed in the water sorption test to show how the water stability was impacted by the monomer structures (vide infra).

In situ photocuring kinetics of the CuAAC polymerization featuring AK/AZ-1 monomers and the photopolymerization of BisGMA/TEGDMA was investigated using FT-IR under continuous irradiation using 400-500 nm visible light with the light intensity set at 200 mW cm<sup>-2</sup>. (See Supporting information Fig. S1). The BisGMA/TEGDMA resin reacted immediately upon light exposure, achieving maximum conversion in about 15 s, while the CuAAC resin showed slower but comparable kinetics, primarily because of the rate-limiting character of the copper(II) reduction step after radical formation upon light exposure, achieving its maximum conversion in about 30 s. The maximum conversion for the CuAAC polymerization with AK/AZ-1 was much higher than that of the dimethacrylate polymerization with BisGMA/TEGDMA (91% vs 66%), and in both cases non-complete maximum conversions were the result of vitrification given that the  $T_g$  values for both resins were much higher than ambient temperature (Table 1). Nonetheless, delayed gelation in the step-growth CuAAC polymerization contributed to the much higher final conversion in comparison to the dimethacrylate polymerization, in which early onset of gelation and vitrification significantly limited the mobility of the reactive species and led to relatively low final conversion. In addition, the polymerization-induced shrinkage stress of the CuAAC polymerization of AK and AZ-1 monomers was much lower than that of the radical polymerization of BisGMA/TEGDMA resin, similar to what was previously observed with the AK/AZ-3 system (see Ref. [27]).



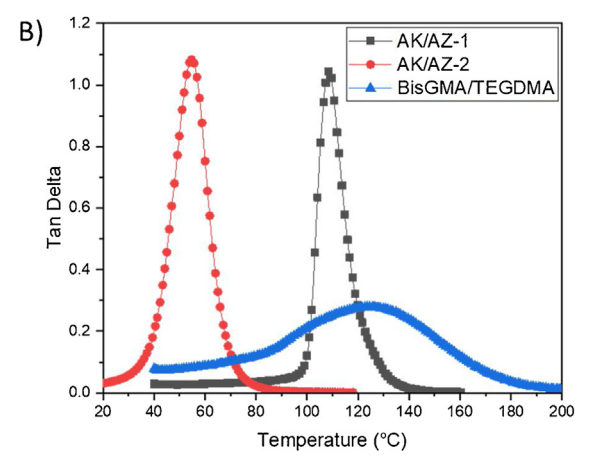


Fig. 2 – Thermomechanical properties of the two CuAAC networks AK/AZ-1 and AK-AZ-2, and the poly(methacrylate) network based on BisGMA/TEGDMA. (A) Plot of storage modulus vs temperature. (B) Tan delta vs temperature.

Table 1 – FT-IR spectrometer and tensometer were used to measure functional group conversions and in situ shrinkage stress during photocuring. Dynamic mechanical analysis (DMA) was used to measure the storage modulus at 40 °C (E' $_{40}$ °C), and glass transition temperature (Tg) of the photo-polymerized films. Bulk photo-CuAAC polymer denoted as AK/AZ-1 and dimethacrylate-based polymer denoted as BisGMA/TEGDMA were compared. Within each row, the letters indicate statistically significant differences (p < 0.05) via a one-way ANOVA and a Tukey's test.

	AK/AZ-1	BisGMA/TEGDMA
Conversion [%]	$93\pm2^{\text{A}}$	$66 \pm 1^B$
T <sub>g</sub> [°C]	$108 \pm 2^{\text{A}}$	$128 \pm 3^{\text{B}}$
Storage modulus @ 40 °C [GPa]	$1.4\pm0.2^{\text{A}}$	$1.9\pm0.2^{\text{B}}$
Final shrinkage stress [MPa]	$0.56\pm0.01^{\text{A}}$	$1.0\pm0.0^{\text{B}}$

The shrinkage stress of the AK/AZ-1 system was slightly higher than that of the AK/AZ-3 system (0.56 MPa vs 0.43 MPa), primarily because of the higher crosslink density of AK/AZ-1 network and the earlier gelation of the tri-alkyne/tri-azide system in comparison to the tri-alkyne/di-azide system.

Next, three-point flexural tests were performed on a universal testing machine (MTS) to investigate the flexural properties (flexural modulus, flexural strength, and flexural toughness) of both the AK/AZ-1 CuAAC network and the Bis-GMA/TEGDMA poly(methacrylate) network (Fig. 3). Flexural modulus (E) and flexural strength ( $\sigma$ ) values were calculated using the following Eqs. (1) and (2) [46]:

$$E = \frac{FL^3}{4dBH^3} \tag{1}$$

$$\sigma = \frac{3FL}{2BH^2} \tag{2}$$

where F is the maximum load, L is the length of span, d is the extension corresponding to the load F, B is the width of the sample specimen, and H is the height of the sample specimen.

Calculations based on three-point flexural testing results showed that the flexural modulus of the AK/AZ-1 CuAAC network (2.9 GPa) was about one forth lower than that of the

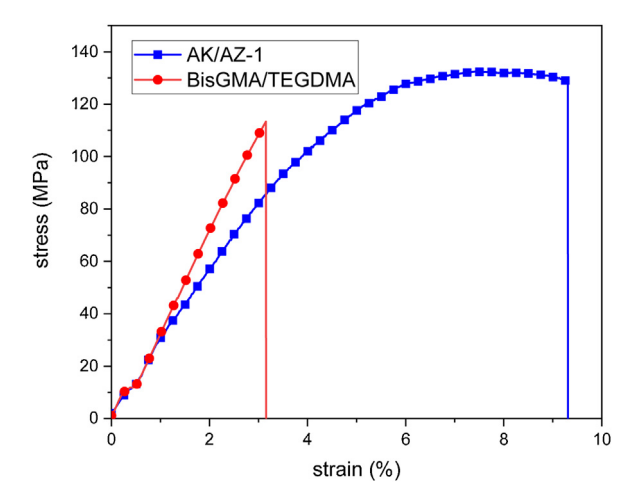
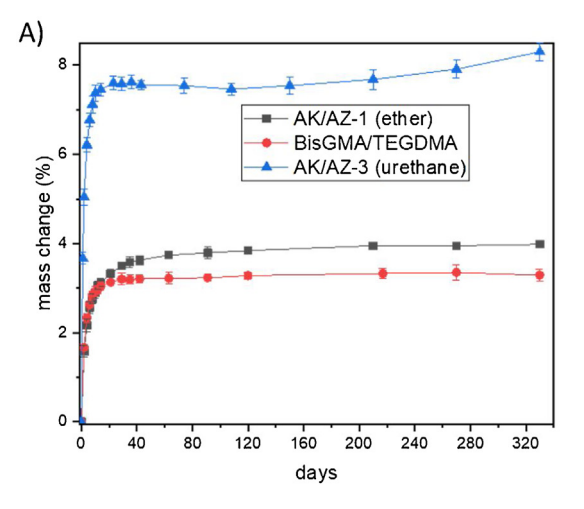


Fig. 3 – Representative stress-strain curves of the AK/AZ-1 CuAAC network and the BisGMA/TEGDMA-based poly(methacrylate) network as measured through three-point flexural tests. Three measurements were conducted for each group of samples. (See Supporting information Fig. S2 for the stress-strain curves of all specimens).

Table 2 – A comparison of flexural modulus (E), flexural strength ( $\sigma$ ), flexural toughness (G<sub>c</sub>) values measured from three-point-bending tests with bulk photo-CuAAC polymer denoted as AK/AZ-1 and dimethacrylate-based polymer denoted as BisGMA/TEGDMA. The letters indicate statistically significant differences (p < 0.05) via a one-way ANOVA and a Tukey's test.

	AK/AZ-1	BISGMA/TEGDMA
Flexural modulus (E) [GPa]	$2.9 \pm 0.3^{\text{A}}$	$3.9 \pm 0.1^{\text{B}}$
Flexural strength (σ) [MPa]	$130\pm10^{\text{A}}$	$110 \pm 10^{\text{B}}$
Flexural toughness ( $G_c$ ) [MJ/ $m^3$ ]	$7.6\pm1.1^{\text{A}}$	$1.6\pm0.3^{\text{B}}$

BisGMA/TEGDMA-based poly(methacrylate) network (3.9 GPa), while the flexural strength of the AK/AZ-1 network was about 10% higher (130 MPa vs 110 MPa) (Table 2). Approximately 7.6



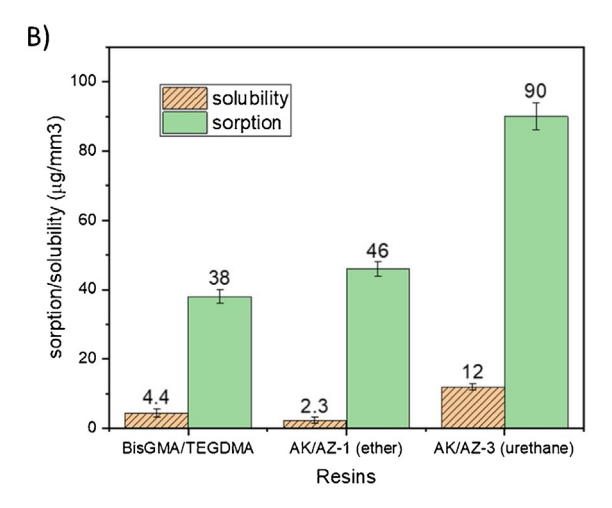


Fig. 4 – Results from the water sorption/solubility tests of BisGMA/TEGDMA network and AK/AZ-1 and AK/AZ-3 CuAAC networks. (A) Sample mass increase against water conditioning time (days). (B) Water sorption/solubility values calculated.

MJ/m<sup>3</sup> of energy was absorbed by the AK-AZ-1 network before the fracture of the samples, which was more than four times the value of the BisGMA/TEGDMA-based network before fracture, highlighting the high toughness of the CuAAC networks in contrast to the brittleness of the poly(methacrylate) network.

Finally, the water sorption/solubility test was conducted with AK/AZ-1 and AK/AZ-3 CuAAC networks and the Bis-GMA/TEGDMA network to compare the water stabilities of the CuAAC networks and the poly(methacrylate) network and to investigate how the water stability of the CuAAC networks was affected by the monomer structure. For the urethane-based AK-AZ-3 CuAAC network, the water uptake sharply increased within the first 2 weeks of water conditioning and plateaued after about 3 weeks at around of 7.6 wt.% swelling, while for the ether-based AK/AZ-1 CuAAC network and the BisGMA/TEGDMA network, the water uptake was much slower and plateaued after about 2 months at much lower levels, with the AK/AZ-1 CuAAC network reaching a swelling of about 3.9 wt.% and the BisGMA/TEGDMA network reaching a swelling of about 3.3 wt.% (Fig. 4A). Compared with the BisGMA/TEGDMA network, the water uptake of the ether-based AK/AZ-1 CuAAC network was only 20% higher but saw a 50% reduction in comparison to the urethanebased AK/AZ-3 CuAAC network, highlighting the value of the hydrophobic ether groups and higher crosslink density of the network in suppressing the water uptake. Similar results were obtained by comparing the calculated water sorption values for the three networks (Fig. 4B). Despite the slightly higher water sorption of the AK/AZ-1 network, the value of its water solubility was only about half the value of the BisGMA/TEGDMA network's water solubility, highlighting the benefits of the higher final conversion of the AK/AZ-1 network in diminishing the leaching of the resin. For the urethane-based AK/AZ-3 network, however, because of the high level of water swelling, much of the unbonded species (copper catalyst, ligands, initiator fragments, trace of unreacted monomers) became leachable and contributed to its high water-sorption.

### 5. Conclusions

Ester-free ether-based monomers of photo-CuAAC polymerization were evaluated as dental restorative resins by examining the mechanical properties and water stabilities in comparison to the commercially available BisGMA/TEGDMA resin. The ether-based AK/AZ-1 CuAAC network exhibited a lower glass-transition temperature (108 °C vs 128 °C), but because of its much sharper glass transition, the AK/AZ-1 network maintained a storage modulus higher than 1 GPa up to 100 °C while the BisGMA/TEGDMA network saw a significant decrease of storage modulus at that temperature due to its network inhomogeneity. In addition, the AK/AZ-1 network exhibited reduced shrinkage stress (0.56 MPa vs 1.0 MPa) and much higher flexural toughness (7.6 MJ/m<sup>3</sup> vs 1.6 MJ/m<sup>3</sup>) while showing slightly lower flexural modulus and slightly higher flexural strength compared with the BisGMA/TEGDMA network. Moreover, the ether-based AK/AZ-1 network developed here displayed comparable water stability in comparison to the BisGMA/TEGDMA network with slightly higher water sorption (46 μg/mm<sup>3</sup> vs 38 μg/mm<sup>3</sup>) and much lower water solubility (2.3  $\mu$ g/mm<sup>3</sup> vs 4.4  $\mu$ g/mm<sup>3</sup>). Compared with the previously developed urethane-based AK/AZ-3 network, water stability of the ether-based AK/AZ-1 network was significantly improved, further paving the way for photo-CuAAC polymer networks to be applied as an alternative to the currently widely used methacrylate dental restorative resins.

# Acknowledgment

The authors acknowledge financial support from the National Science Foundation CHE 1808484.

# Appendix A. Supplementary data

Supplementary material related to this article can be found, in the online version, at doi:https://doi.org/10.1016/j.dental.2021.08.010.

### REFERENCES

- [1] Ferracane JL. Current trends in dental composites. Crit Rev Oral Biol Med 1995;6(4):302–18, http://dx.doi.org/10.1177/10454411950060040301.
- [2] Cramer NB, Stansbury JW, Bowman CN. Recent advances and developments in composite dental restorative materials. J Dent Res 2011;90(4):402–16, http://dx.doi.org/10.1177/0022034510381263.
- [3] Davy KW, Braden M. Study of polymeric systems based on 2,2-bis-4(2-hydroxy-3methacryloyloxypropoxy)phenylpropane. Biomaterials 1991;12:406–41, http://dx.doi.org/10.1016/0142-9612(91)90009-y.
- [4] Anseth KS, Newman SM, Bowman CN. Polymeric dental composites: properties and reaction behavior of multimethacrylate dental restorations. Adv Polym Sci 1995;122:177–217, doi:110.1007/3540587888\_16.
- [5] Gonçalves F, Kawano Y, Pfeifer C, Stansbury JW, Braga RR. Influence of BisGMA, TEGDMA, and BisEMA contents on viscosity, conversion, and flexural strength of experimental resins and composites. Eur J Oral Sci 2009;117:442–6, http://dx.doi.org/10.1111/j.1600-0722.2009.00636.x.
- [6] Sadowsky SJ. An overview of treatment considerations for esthetic restorations: a review of the literature. J Prosthet Dent 2006;96:433–42, http://dx.doi.org/10.1016/j.prosdent.2006.09.018.
- [7] Ruyter IE, Svendsen SA. Remaining methacrylate groups in composite restorative materials. Acta Odontol Scand 1978:75–82, http://dx.doi.org/10.3109/00016357809027569.
- [8] Patel MP, Braden M, Davy KWM. Polymerization shrinkage of methacrylate esters. Biomaterials 1987;8:53–6, http://dx.doi.org/10.1016/0142-9612(87)90030-5.
- [9] Lu H, Stansbury JW, Bowman CN. Towards the elucidation of shrinkage stress development and relaxation in dental composites. Dent Mater 2004;20:979–86, http://dx.doi.org/10.1016/j.dental.2004.05.002.
- [10] Ferracane JL. Developing a more complete understanding of stresses produced in dental composites during polymerization. Dent Mater 2005;21:36–42, http://dx.doi.org/10.1016/j.dental.2004.10.004.
- [11] Braga RR, Ballester RY, Ferracane JL. Factors involved in the development of polymerization shrinkage stress in resin-composites: a systematic review. Dent Mater 2005;21:962–70, http://dx.doi.org/10.1016/j.dental.2005.04.018.
- [12] Drummond JL. Degradation, fatigue, and failure of resin dental composite materials. J Dent Res 2008;87:710–9, http://dx.doi.org/10.1177/154405910808700802.
- [13] Kolin PJ, Kilislioglu A, Zhou M, Drummond JL, Hanley L. Analysis of the degradation of a model dental composite. J Dent Res 2008;87:661–5, http://dx.doi.org/10.1177/154405910808700712.
- [14] Gonzalez-Bonet A, Kaufman G, Yang Y, Wong C, Jackson A, Huyang G, et al. Preparation of dental resins resistant to enzymatic and hydrolytic degradation in oral environments. Biomacromolecules 2015;16(10):3381–8, http://dx.doi.org/10.1021/acs.biomac.5b01069.
- [15] Yapa AUJ, Lee HK, Sabapathy R. Release of methacrylic acid from dental composites. Dent Mater 2000;16(3):172–9, http://dx.doi.org/10.1016/S0109-5641(00)00004-X.
- [16] Santerre JP, Shajii L, Leung BW. Relation of dental composite formulations to their degradation and the release of hydrolyzed polymeric-resin-derived products. Crit Rev Oral Biol Med 2001;12(2):136–51, http://dx.doi.org/10.1177/10454411010120020401.

- [17] Szczepanska J, Poplawsk T, Synowiec E, Pawlowska E, Chojnacki CJ, Chojnacki J, et al. 2-Hydroxylethyl methacrylate (HEMA), a tooth restoration component, exerts its genotoxic effects in human gingival fibroblasts trough methacrylic acid, an immediate product of its degradation. Mol Biol Rep 2012;39:1561–74, http://dx.doi.org/10.1007/s11033-011-0895-y.
- [18] Weinmann W, Thalacker C, Guggenberger R. Siloranes in dental composites. Dent Mater 2005;21:68–74, http://dx.doi.org/10.1016/j.dental.2004.10.007.
- [19] Eick JD, Kotha SP, Chappelow CC, Kilway KV, Giese GJ, Glaros AG, et al. Properties of silorane-based dental resins and composites containing a stress-reducing monomer. Dent Mater 2007;23(8):1011–7, http://dx.doi.org/10.1016/j.dental.2006.09.002.
- [20] Lien W, Vandewalle KS. Physical properties of a new silorane-based restorative system. Dent Mater 2010;26(4):337–44, http://dx.doi.org/10.1016/j.dental.2009.12.004.
- [21] Hoyle CE, Bowman CN. Thiol-ene click chemistry. Angew Chem Int Ed 2010;49:1540-73, http://dx.doi.org/10.1002/anie.200903924.
- [22] Lowe AB. Thiol-ene "click" reactions and recent applications in polymer and materials synthesis. Polym Chem 2010;1:17–36, http://dx.doi.org/10.1039/B9PY00216B.
- [23] Carioscia JA, Lu H, Stansbury JW, Bowman CN. Thiol-ene oligomers as dental restorative materials. Dent Mater 2005;21:1137–43, http://dx.doi.org/10.1016/j.dental.2005.04.002.
- [24] Cramer NB, Couch CL, Schreck KM, Carioscia JA, Boulden JE, Stansbury JW. Investigation of thiol-ene and thiol-ene-methacrylate based resins as dental restorative materials. Dent Mater 2010;26:21–8, http://dx.doi.org/10.1016/j.dental.2009.08.004.
- [25] Podgórski M, Becka E, Claudino M, Flores A, Shah PK, Stansbury JW, et al. Ester-free thiol-ene dental restoratives—part A: resin development. Dent Mater 2015;31:1255-62,
  - http://dx.doi.org/10.1016/j.dental.2015.08.148.
- [26] Khatri CA, Stansbury JW, Schultheisz CR, Antonucci JM. Synthesis, characterization and evaluation of urethane derivatives of Bis-GMA. Dent Mater 2003;19:584–8, http://dx.doi.org/10.1016/S0109-5641(02)00108-2.
- [27] Ge J, Trujillo M, Stansbury JW. Synthesis and photopolymerization of low shrinkage methacrylate monomers containing bulky substituent groups. Dent Mater 2005;21:1163–9, http://dx.doi.org/10.1016/j.dental.2005.02.002.
- [28] Atai M, Ahmadi M, Babanzadeh S, Watts DC. Synthesis, characterization, shrinkage and curing kinetics of a new low-shrinkage urethane dimethacrylate monomer for dental applications. Dent Mater 2007;23:1030–41, http://dx.doi.org/10.1016/j.dental.2007.03.004.
- [29] Moszner N, Fischer UK, Angermann J, Rheinberger V. A partially aromatic urethane dimethacrylate as a new substitute for Bis-GMA in restorative composites. Dent Mater 2008;24:694–9, http://dx.doi.org/10.1016/j.dental.2007.07.001.
- [30] Leung D, Bowman CN. Reducing shrinkage stress of dimethacrylate networks by reversible addition-fragmentation chain transfer. Macromol Chem Phys 2012;213:198–204, http://dx.doi.org/10.1002/macp.201100402.
- [31] Park HY, Kloxin CJ, Abuelyaman AS, Oxman JD, Bowman CN. Novel dental restorative materials having low polymerization shrinkage stress via stress relaxation by addition-fragmentation chain transfer. Dent Mater 2012;28:1113–9, http://dx.doi.org/10.1016/j.dental.2012.06.012.

- [32] Park HY, Kloxin CJ, Fordney MF, Bowman CN. Stress relaxation of trithiocarbonate-dimethacrylate-based dental composites. Dent Mater 2012;28:888–93, http://dx.doi.org/10.1016/j.dental.2012.04.016.
- [33] Kolb HC, Finn MG, Sharpless KB. Click chemistry: diverse chemical function from a few good reactions. Angew Chem Int Ed 2001;40:2004–21, http://dx.doi.org/10.1002/1521-3773(20010601)40:11.
- [34] Moses JE, Moorhouse AD. The growing applications of click chemistry. Chem Soc Rev 2007;36:1249–62, http://dx.doi.org/10.1039/B613014N.
- [35] Xi W, Scott TF, Kloxin CJ, Bowman CN. Click chemistry in materials science. Adv Funct Mater 2014;24:2572–90, http://dx.doi.org/10.1002/adfm.201302847.
- [36] Tornøe CW, Christensen C, Meldal M. Peptidotriazoles on solid phase: [1,2,3]-triazoles by regiospecific copper(I)-catalyzed 1,3-dipolar cycloadditions of terminal alkynes to azides. J Org Chem 2002;67:3057–64, http://dx.doi.org/10.1021/jo011148j.
- [37] Rostovtsev VV, Green LG, Fokin VV, Sharpless KB. A stepwise Huisgen cycloaddition process: copper(I)-catalyzed regioselective "ligation" of azides and terminal alkynes. Angew Chem Int Ed 2002;41:2596–9, http://dx.doi.org/10.1002/1521-3757(20020715)114:14.
- [38] Adzima BJ, Tao Y, Kloxin CJ, DeForest CA, Anseth KS, Bowman CN. Spatial and temporal control of the alkyne-azide cycloaddition by photoinitiated Cu(II) reduction. Nat Chem 2011;3:256–9, http://dx.doi.org/10.1038/NCHEM.980.
- [39] Tasdelen MA, Yilmaz G, Iskin B, Yagci Y. Photoinduced free radical promoted copper(I)-catalyzed click chemistry for macromolecular syntheses. Macromolecules 2012;45:56–61, http://dx.doi.org/10.1021/ma202438w.

- [40] Song HB, Wang X, Patton JR, Stansbury JW, Bowman CN. Kinetics and mechanics of photo-polymerized triazole-containing thermosetting composites via the copper(I)-catalyzed azide-alkyne cycloaddition. Dent Mater 2017;33:621-9, http://dx.doi.org/10.1016/j.dental.2017.03.010.
- [41] Song HB, Sowan N, Shah PK, Baranek A, Flores A, Stansbury JW, et al. Reduced shrinkage stress via photo-initiated copper(I)-catalyzed cycloaddition polymerizations of azide-alkyne resins. Dent Mater 2016;32:1332–42, http://dx.doi.org/10.1016/j.dental.2016.07.014.
- [42] Song HB, Baranek A, Worrell BT, Cook WD, Bowman CN. Photopolymerized triazole-based glassy polymer networks with superior tensile toughness. Adv Funct Mater 2018;28:1801095, http://dx.doi.org/10.1002/adfm.201801095.
- [43] Baranek A, Song HB, McBride M, Finnegan P, Bowman CN. Thermomechanical formation-structure-property relationships in photopolymerized copper-catalyzed azide-alkyne (CuAAC) networks. Macromolecules 2016;49:1191-200, http://dx.doi.org/10.1021/acs.macromol.6b00137.
- [44] Sideridou I, Achilias DS, Spyroudi C, Karabela M. Watersorption characteristics of light-cured dental resins and composites based on Bis-EMA/PCDMA. Biomaterials
  - 2004;25:367-76, http://dx.doi.org/10.1016/s0142-9612(03)00529-5.
- [45] Shete AU, El-Zaatari BM, French JM, Kloxin CJ. Blue-light activated rapid polymerization for defect-free bulk Cu(I)-catalyzed azide–alkyne cycloaddition (CuAAC) crosslinked networks. Chem Commun 2016;52:10574–7, http://dx.doi.org/10.1039/C6CC05095F.
- [46] Rodrigues Junior SA, Zanchi CH, de Carvalho RV, Demarco FF. Flexural strength and modulus of elasticity of different types of resin-based composites. Braz Oral Res 2007;21:16–21, http://dx.doi.org/10.1590/S1806-83242007000100003.